

## OBSERVATIONS OF SHEAR-COUPLED P WAVES

George Zandt and George E. Randall

Department of Geological and Environmental Sciences  
State University of New York at Binghamton

**Abstract.** Teleseismic SV waves couple to P waves in the lithosphere in several ways. P waves converted from discontinuities in the lithosphere precede the main SV arrival as small amplitude Sp precursors. Large amplitude P waves follow the main SV arrival after conversion by reflection at the free surface, and post-critical reflection from a discontinuity in the lithosphere. SPdiff denotes a converted P wave diffracted along the underside of the crust when a teleseismic SV wave strikes it from below near the critical angle of incidence.

We observed several of these shear-coupled P waves on seismograms of deep earthquakes recorded at broadband seismic stations (RSTN) in North America. For these paths, large amplitudes relative to SV characterize the lithospheric multiple near 50°, with amplitudes decreasing rapidly beyond 60°. Calculation of synthetic seismograms indicate that a post-critical reflection from a discontinuity at 70-80 km depth where compressional velocity increases abruptly to about 8.5 km/s produce the largest amplitude P arrival. The observations of these shear-coupled P waves presents a previously untapped source of information about the fine structure of the upper mantle.

## Introduction

At teleseismic distances, the vertically polarized shear (SV) waveforms appear more complicated than the corresponding compressional (P) waveforms because the S-to-P conversions at discontinuities and at the free surface refract away from the vertical, sometimes leading to critical reflection and refraction phenomena. **Converted P waves can arrive before the S wave or follow it after an additional pre- or post-critical reflection from a deeper layer.** In addition, the converted P wave generated below a discontinuity at a critical angle of incidence, can propagate like an interference head wave to large distances.

The raypaths for important converted phases for a one layer crust are illustrated in the top of Figure 1. For simplicity the schematic raypaths start at the same position and end at different stations; of course, for a single station these waves would be generated at varying distances from the receiver. The S-to-P conversion at the base of the crust, Sp, arrives before the main S phase; Jordan and Frazer (1975) studied this phase to determine crustal structure in eastern Canada. A converted P wave reflected back up from the base of the crust follows the main S wave. Using the notation of Bath and Stefansson (1966), this phase is denoted SsPmP; however, we refer to it simply as SPmP. Although much weaker in amplitude, the phase SpSmP has the same travel time and adds

constructively to SPmP. We are not aware of any previous studies of these reflections as discrete body wave phases in the teleseismic SV coda.

The critical distance for SPmP (about 50°) separates post-critical reflections at shorter ranges from pre-critical reflections at larger ranges; the opposite order in comparison to a surface source seismic survey, because teleseismic waves emerge more steeply as range increases. In post-critical reflection the free surface converted P wave is totally reflected and trapped in the crust except for the energy leaking out of the layer as converted S waves. In contrast, the pre-critical reflection transmits P energy into deeper layers. Therefore, the SPmP wave exhibits large amplitude and a Hilbert transform type phase shift for distances shorter than critical, and small amplitude and simple waveform at larger distances. In addition, constructive interference of post-critically trapped waves produces the SPL wave, a dispersive leaky mode prominent on long period records of shallow earthquakes and studied by Frazer (1977) and Baag and Langston (1985).

Another complication occurs when the incident S wave emerges at the base of the crust at the critical angle for the P wave converted below the Moho. This grazing P wave propagates like a head wave and is called the SPdiff phase (Figure 1). First synthesized and recognized by Frazer (1977) in his thesis on the shear-coupled PL wave, the diffracted wave emerges at large distances (80° to 100°) if the upper mantle velocity gradient is appropriate to set up a whispering gallery. Frazer (1977), not finding any observations of this wave in Canada, concluded that a negative velocity gradient characterizes the upper mantle beneath the Canadian Shield. Recently, Baag and Langston (1984) reported observations of this phase in data from the Australian Shield.

The variety of shear-coupled P waves we described contribute to the complexity of long period SV waves, an effect commonly cited in the seismological literature. We have identified some of these SV-coupled P waves from several deep South American earthquakes recorded on broadband seismic stations in North America. These waves appear very impulsive on the broadband records, therefore we were able to make accurate travel time measurements and waveform comparisons. A

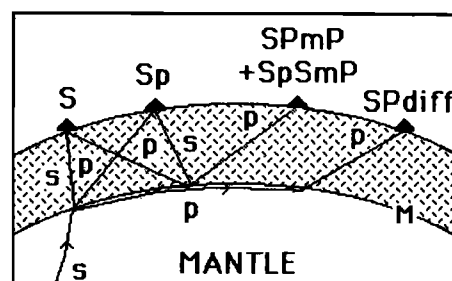


Fig. 1. Schematic raypaths for crustal P waves coupled to teleseismic SV wave.

Copyright 1985 by the American Geophysical Union.

Paper number 5L6609.  
0094-8276/85/005L-6609\$03.00

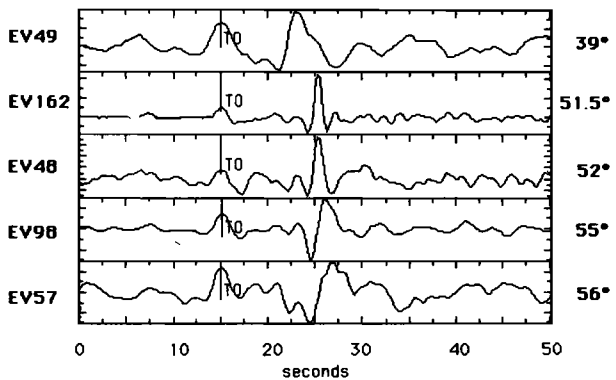


Fig. 2. SV waveforms (vertical component) recorded at RSCP from deep focus events. Traces are aligned along SV arrivals ( $T_0$ ). Indicated depths are corrected to a common depth of 30 km.

major result of this study is the discovery of a converted P wave reflection from an upper mantle discontinuity beneath eastern North America.

#### Broadband SV Waveforms

The Regional Seismic Test Network (RSTN), a group of five broadband seismic stations located in North America and operated by the Department of Energy (Taylor and Qualheim, 1982), recorded the data used in this study. We first observed the P phase within the SV waveform of five deep South American earthquakes recorded on the mid-period passband of station RSCP ( $35^{\circ} 36.0' N$ ,  $85^{\circ} 34.1' W$ , Tennessee). The vertical component seismograms of these events are plotted in Figure 2 in order of increasing distance. The event numbers at the beginning of each trace correspond to the source parameters listed in Table 1. Each trace was normalized to the SV wave amplitude with the distances corrected to a common source depth of 30 km. We are interested in the large impulsive arrivals following the SV wave by 8 to 12 seconds.

The vertical and radial seismograms and a particle motion diagram for the event at  $55^{\circ}$ , displayed in Figure 3, aids in phase identification. An Sp wave identified in this seismogram at about 7.5 seconds before SV has the appropriate lead time for a conversion at the base of a 45 km thick crust, in agreement with other estimates for this location (Owens et al., 1984; Prodehl et al., 1984). A P wave arriving at an angle of incidence of about  $45^{\circ}$  constitutes the large secondary phase about 11 seconds after the SV wave. Its arrival near but after the S wave indicates generation near the receiver and points to a reflected conversion such as SPmP.

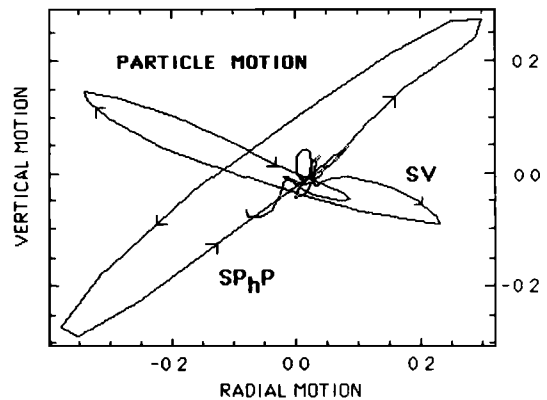
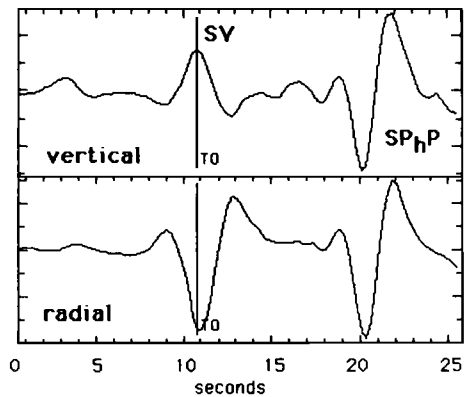


Fig. 3. SV waveform of event 98 (range =  $55^{\circ}$ ) recorded at RSCP (Top). Particle motion diagram of the traces showing SV- and P- motions (Bottom).

In order to test this possibility, we computed synthetic seismograms using the Thomson-Haskell method (Haskell, 1962). Figure 4 shows the comparison of the data (middle panel) with a synthetic seismogram for a 45 km thick crust (top panel). The SPmP phase in the synthetic arrives a few seconds too early to match the data, and at this range the reflection is pre-critical and too small in amplitude in comparison to the observed phase. With the addition of a deeper discontinuity in the model (velocity increase to 8.5 km/s at 75 km depth, see Table 2) a post-critical reflection from the deeper layer becomes possible (see ray-path sketch in Figure 4). The synthetic seismogram for this case matches the data much more closely (compare middle and bottom panels of Figure 4). We conclude that a small pre-critical SPmP reflection and a large post-critical reflection, denoted SP<sub>h</sub>P, from a 75 km deep velocity discontinuity combine to create the large P wave in the SV waveform.

TABLE 1. Event Information

Event	Date	Origin Time	Depth	Delta <sup>1</sup>	BAZ <sup>1</sup>	Region
48	Sep 15, 1982	20h 22m 55.2s	128 km	51.8°	161.6°	Peru
49	Nov 18, 1982	14h 57m 52.4s	195 km	38.0°	165.5°	Ecuador
57	Feb 25, 1983	22h 49m 54.7s	146 km	55.7°	161.3°	N. Chile
98	Feb 26, 1984	08h 18m 19.8s	113 km	54.5°	162.3°	Peru
162	Jun 02, 1983	20h 12m 50.7s	599 km	46.9°	160.6°	Peru-Brazil

<sup>1</sup> with respect to RSCP

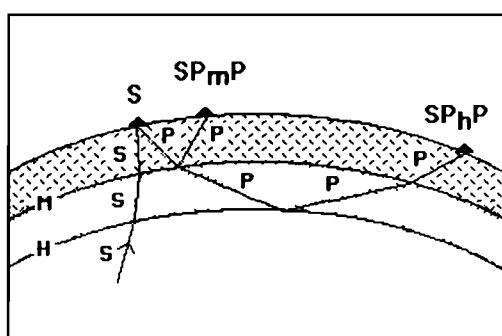
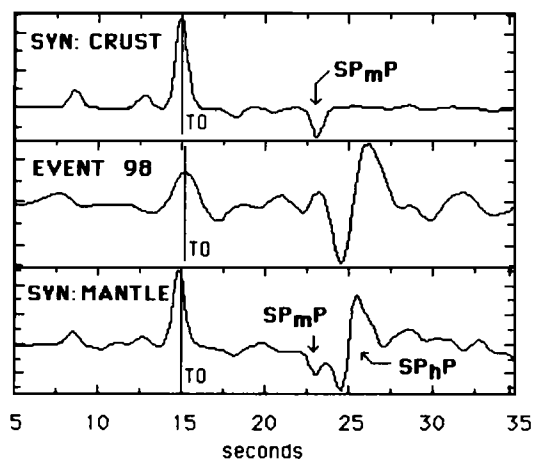


Fig. 4. Comparison of event 98 (middle) with synthetics for a simple crustal model (top) and one with an upper mantle discontinuity (bottom). Below is a schematic picture of raypaths for the two reflections indicated on the traces.

If this identification is correct we should observe significant waveform variations on seismograms recorded at distances straddling the  $SP_mP$  critical distance of about  $50^\circ$ . This effect is demonstrated in Figure 5 which compares the deconvolved vertical components with the corresponding Thomson-Haskell synthetics for various distances. Deconvolution was done by spectral division with the SH waveform or the windowed SV waveform. At  $39^\circ$ , before the critical distance,  $SP_mP$  is totally reflected, producing a large amplitude, phase shifted waveform with no deeper reflection. At  $52^\circ$ , beyond the critical distance,  $SP_mP$  leaks some of its energy through the base of the crust; hence, it becomes smaller in amplitude and the totally reflected wave from the deeper layer dominates the record. At larger distances the  $SP_hP$  waveform changes in response to post-critical phase changes that are dependent on angle of incidence. Although not shown, beyond the  $SP_hP$

TABLE 2. Velocity Model for RSCP

VP (km/s)	VS (km/s)	Thickness (km)
6.1	3.52	15.
6.9	3.98	30.
8.0	4.62	30.
8.5	4.91	Halfspace

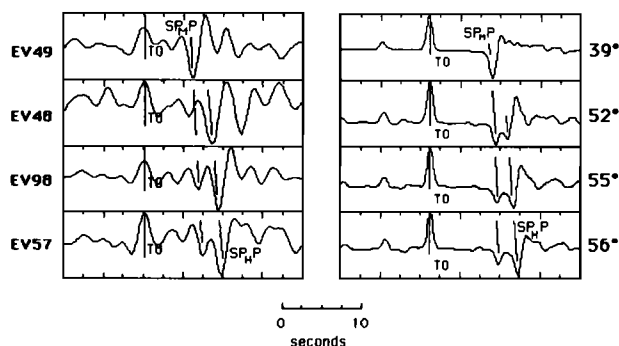


Fig. 5. Comparison of deconvolved vertical component seismograms (left panels) and corresponding synthetics (right panels) for a velocity model with a high velocity halfspace.

critical distance, the reflection becomes pre-critical and decays rapidly in amplitude with increasing distance. Considering the simplicity of the model, the synthetic waveforms are quite similar to the data, lending credence to our identification of these P waves as reflections from the base of the crust and reflections from an upper mantle discontinuity at about 75 km depth where the P velocity increases to about 8.5 km/s.

Data become sparse for distances beyond about  $60^\circ$ . However, on the limited data we continue to observe P waves in the SV waveform out to  $90^\circ$ , well beyond where  $SP_hP$  should remain prominent. These later P waves have smaller amplitudes and post-SV arrival times that range from about 20 to 70 seconds, increasing with range. Possible identifications of these P waves include the surface reflection SP,  $SP_{diff}$  from the base of the crust,  $SP_{diff}$  from the deeper discontinuity, or deeper reflections. Verification of one of these interpretations awaits analysis of more data.

#### Discussion

Examination of Figure 5 reveals some important differences between the data and the synthetic seismograms. The P wave to S wave amplitude ratio is much smaller in the synthetic than in the observed seismograms. The ratio can not be increased simply by increasing the velocity contrast at the deep discontinuity because the post-critical reflection is totally reflected; varying the contrast does affect the phase angle for post-critical reflections. Also, the critical distance sharply truncates the synthetic reflection from the deeper discontinuity; whereas in the data the phase appears to 'leak' into the post-critical region.

These differences may be due in part to the inadequacy of the plane wave coefficients in the Thomson-Haskell synthetics. Richards (1976) demonstrated this inadequacy for waves interacting with discontinuities at or near grazing angles of incidence and developed the full wave theory (Richards, 1973; Cormier and Richards, 1977) to properly model these waves. In the modified theory the reflection and transmission coefficients become frequency dependent and waveforms change more gradually near the critical angle of incidence than predicted by ray theory. The Thomson-Haskell synthetics also assume homogeneous layers; perhaps gradients or alternating velocity layers could affect the amplitude ratio. We have not yet made extensive modeling efforts to get a

better fit. Despite these differences, the overall comparison is favorable enough for us to conclude that a major upper mantle discontinuity exists at a depth of 70 to 80 km beneath RSCP.

Independent evidence indicates that this upper mantle discontinuity is a regional feature of at least the eastern North American lithosphere. Hales (1969) reviewed the Early Rise refraction experiment in which large explosions in Lake Superior were recorded along several long profiles radiating from the Lake. On both northern and southern profiles, a first arriving phase with an apparent velocity of 8.5 to 8.6 km/s emerges at about 650 km. Hales and others have interpreted this phase as a refraction from a discontinuity at a depth of 80 to 90 km.

Hales (1969) originally suggested that the discontinuity may arise as a result of a transition from spinel to garnet peridotite; later, Hales et al. (1970) suggested the second stage of the gabbro to eclogite transition in which garnet is developed causes this discontinuity. Fuchs and Vinnik (1981) reviewed a number of European and Soviet long-range seismic profiles in which high velocity layers of up to 8.6 - 8.7 km/s were detected in the upper mantle at depths less than 100 km. According to their interpretation, the high-velocity layering in the uppermost mantle is due to velocity anisotropy induced by preferred orientation of olivine. The petrological or tectonic interpretation of high velocities ( $V_p \sim 8.5$  km/s) in the upper 100 km of the mantle remains uncertain and poses an important problem in geodynamics.

In summary, we have identified the P wave arrivals following the SV wave in the range  $35^\circ$  to  $60^\circ$  as converted waves reflecting from crustal and upper mantle discontinuities. This observation opens up the possibility of studying the regional P wave structure in an area devoid of regional earthquakes by taking advantage of teleseismic events recorded at a single three-component station or a regional network of such stations.

**Acknowledgements.** This work was supported by NSF grant EAR-8319652. Computations were performed on our computer system purchased in part from NSF grant EAR-8306562. We would like to especially thank Tom Owens and Steve Taylor for help in data acquisition; Norm Burr, Joe Tull, and Earth Sciences at LLNL for SAC; Charles Langston and Vernon Cormier for helpful discussions; and our colleagues at SUNY-Binghamton for their support.

#### References

- Bath, M., and R. Stefansson, S-P conversion at the base of the crust, Ann. Geofis., 19, 119-130, 1966.
- Cormier, V.F., and P.G. Richards, Full wave theory applied to a discontinuous velocity increase: The inner core boundary, J. Geophys., 43, 3-31, 1977.
- Frazer, N.L., Synthesis of shear-coupled PL, PhD Thesis, 54 pp., Princeton University, NJ, 1977.
- Fuchs, K., and L.P. Vinnik, Investigation of the subcrustal lithosphere and asthenosphere by controlled source seismic experiments on long-range profiles, in Evolution of the Earth, edited by R.J. O'Connell and W.S. Fyfe, 81-98, Geodynamics Series Volume 5, AGU, Washington, D.C., 1981.
- Hales, A.L., A seismic discontinuity in the lithosphere, Earth and Planetary Science Letters, 7, 44-46, 1969.
- Hales, A.L., Helsley, C.E., and J.B. Nation, P travel times for an oceanic path, J. Geophys. Res., 75, 7362-7381, 1970.
- Haskell, N.A., Crustal reflection of plane P and SV waves, J. Geophys. Res., 67, 4751-4767, 1962.
- Jordan, T.J., and L.N. Frazer, Crustal and upper mantle structure from Sp phases, J. Geophys. Res., 80, 1504-1518, 1975.
- Owens, T.J., Zandt, G., and S.R. Taylor, Seismic evidence for an ancient rift beneath the Cumberland Plateau, Tennessee: A detailed analysis of broadband teleseismic P waveforms, J. Geophys. Res., 89, 7783-7795, 1984.
- Prodehl, C., Schlittenhardt, J., and S.W. Stewart, Crustal structure of the Appalachian Highlands in Tennessee, Tectonophysics, 109, 61-76, 1984.
- Richards, P.G., Calculation of body waves for caustics and tunnelling in core phases, Geophys. J. R. Astron. Soc., 35, 243-264, 1973.
- Richards, P.G., On the adequacy of plane-wave reflection/transmission coefficients in the analysis of seismic body waves, Bull. Seismol. Soc. Am., 66, 701-717, 1976.
- Taylor, S.R., and B.J. Qualheim, RSTN site descriptions, Rep. UCID-19769, 79 pp., Lawrence Livermore Natl. Lab., Livermore, Calif., 1983.

G. Zandt and G. E. Randall, Department of Geological and Environmental Sciences, SUNY at Binghamton, Binghamton, NY 13901

(Received June 18, 1985;  
accepted July 5, 1985.)

Baag, C.E., and C.A. Langston, Diffracted Sp generated under Australian Shield, Eos Trans. AGU, 65, 1000, 1984.